Food and Bioprocess Technology (2022) 15:2531–2546
https://doi.org/10.1007/s11947-022-02899-w

ORIGINAL RESEARCH

Development and Characterization of *Froriepia subpinnata* (Ledeb.) Baill Essential Oil and Its Nanoemulsion Using Ultrasound

Seyedeh-Maryam Hasheminya[1] · **Jalal Dehghannya**[1]

Received: 14 February 2022 / Accepted: 1 September 2022 / Published online: 8 September 2022

Abstract

Nanoemulsification of essential oils (EOs) is one of the common techniques that prevent the EO interaction with food components and improve its bioavailability and absorption. In this study, the EO of *Froriepia subpinnata* (Ledeb.) Baill (FSLB) was extracted, and its 28 compounds were identified by the GC-FID and GC–MS analysis. The EO nanoemulsion (EON) was produced using Tween 80 and Span 80 surfactants with high-intensity ultrasound. Various properties of the EON were examined every 15 days for 2 months. The mean particle size (< 100 nm), polydispersity index (PDI) (< 0.3), and zeta potential (−38.89 to −37.21 mV) of the EON were stable for 45 days. Scanning electron microscopy (SEM) illustrated that the obtained nanoparticles were spherical, and their size was smaller than 100 nm. X-ray diffraction (XRD) patterns showed that the crystal order of the EON changed compared to the blank nanoemulsion (BN). Fourier transform infrared (FTIR) spectroscopy demonstrated that hydrogen bonds were formed between the constituents of the EO and the surfactants. Not only was the antioxidant activity of the EON higher than the EO, but this property in the EON was also more stable over time (45 days) than the EO. The EON showed significantly higher antimicrobial activity against *Escherichia coli* and *Staphylococcus aureus* bacteria than the EO. Unlike the EO, the EON maintained the antibacterial properties for 60 days. Overall, the results demonstrated that the FSLB's EO is suitable for use in various food and bio-based industries.

Keywords Anarijeh · Antibacterial · Antioxidant · Nanoencapsulation · Ultrasound

Introduction

Microbial contamination of food products is one of the most critical public health concerns globally and is considered an essential factor in causing economic losses. One of the ways to increase the safety of foods is to use preservative compounds. Despite the extensive use of chemical preservatives to fight against pathogenic microorganisms in foods, their toxic and carcinogenic substances continue to be a significant concern for public health in the world (Hasheminya et al., 2019b; Moghimi et al., 2016). Natural compounds such as essential oils (EOs) are of interest to consumers due to their beneficial properties without the side effects of similar synthetic chemicals. The application of EO in the food industry as an antimicrobial, antioxidant, and preservative is on the rise (Chaudhari et al., 2020; Das et al., 2021). The plants' EO are mixtures of chemical compounds, some of which exhibit natural antimicrobial properties against pathogenic and food-borne bacterial pathogens (Ghaderi-Ghahfarokhi et al., 2016; Hasheminya et al., 2019a; Jemaa et al., 2018; Lou et al., 2017; Moghimi et al., 2016). *Froriepia subpinnata* (Ledeb.) Baill (FSLB), locally called Anarijeh, is mainly spread in southern and central Europe and north of Iran. The leaves of this plant are used in Iran as flavor agents to prepare different food products. The FSLB is an annual plant with white flowers and a height of 20 to 110 cm. In traditional medicine, this plant is used against liver disorders and as a carminative, antispasmodic, diuretic, sedative, and tonic agent (Mirzania et al., 2019; Mohammadzadeh et al., 2018). However, scientific research about the FSLB is limited, and only a few studies have reported its antimicrobial and antioxidant activity (Mirzania et al., 2019; Mohammadzadeh et al., 2018). Mirzania et al. (2019) investigated the antibacterial and antifungal activity of the FSLB's EO obtained from wild and cultivated samples against *Staphylococcus aureus*, *Enterococcus faecalis*, *Escherichia coli*, *Pseudomonas aeruginosa*, *Candida albicans*, and *Aspergillus flavus*. The results showed that the

✉ Jalal Dehghannya
J_dehghannya@tabrizu.ac.ir

[1] Department of Food Science and Technology, University of Tabriz, Tabriz 51666-16471, Iran

minimum inhibitory concentration (MIC) of the EO against these microorganisms ranged between 1 and 64 µg/mL. The antioxidant and antimicrobial activity of the FSLB's EO is linked to the significant oxygenated monoterpene compounds (Mehrabanjoubani et al., 2021; Mirzania et al., 2019).

Usage of the EO is associated with difficulty in their application due to their water insolubility and physicochemical instability. Besides, the EO creates odor and taste in food products, which is usually not pleasant. Therefore, today, efforts are being made to reduce the adverse effects of the EO in food materials (Hasheminya et al., 2019b; Jemaa et al., 2018; Lou et al., 2017; Salvia-Trujillo et al., 2013). Nanoemulsification of the EO is one of the common methods that significantly disperse the EO in aqueous solutions. Nanoemulsification also prevents the interaction of the EO with food ingredients and improves its absorption and bioavailability (Jemaa et al., 2018; Lou et al., 2017). Also, the EO nanoemulsion (EON) will be helpful for the industry in counteracting bacterial resistance (Jemaa et al., 2018). For instance, due to their larger surface area and smaller size, the EON's antimicrobial activity is enhanced in nanoemulsion-based delivery systems (Moghimi et al., 2016; Salvia-Trujillo et al., 2013; Sepahvand et al., 2021).

Nanoemulsions are prepared from oil, water, and emulsifiers with particle sizes in the range of 10–100 nm (Shahavi et al., 2016). Nanoemulsions are made using high-energy mixing, homogenization, ultrasonication, and microfluidization. These procedures rapidly provide the required energy with a uniform flow to yield droplets of smaller sizes. Ultrasound-assisted extraction has extensively been used in different food and medicinal industries (Hasheminya & Dehghannya, 2020b). Ultrasonication is an appropriate emulsification method during which, by increasing energy consumption, the size of the emulsion droplets is decreased with minimal recoalescence (Ezhilarasi et al., 2013). This method is an efficient and fast technique for producing nanoemulsions with high stability, small droplet size, and suitable polydispersity characteristic. In an ultrasonic probe homogenizer, acoustic cavitation is generated by powerful shock waves to disrupt coarse droplets. Ultrasonication, compared to mechanical agitation techniques, consumes lower energy, needs smaller magnitudes of emulsifiers, and produces droplet sizes with more uniformity and stability (Hasheminya & Dehghannya, 2020b; Shahavi et al., 2016). For example, Sivakumar et al. (2014) used three techniques, namely, magnetic stirring, high-speed homogenization, and ultrasonic emulsification to produce nanoemulsions of aspirin. The results showed that the droplet size of the emulsions of aspirin produced by magnetic stirring, high-speed homogenization, and ultrasonic emulsification was 1160, 359, and 232 nm, respectively. Moreover, the polydispersity index (PDI) of the nanoemulsions produced by magnetic stirring, high-speed homogenization, and ultrasonic emulsification methods was reported as 0.971, 0.379, and 0.309, respectively. In another study, Gavahian et al. (2018) used conventional power ultrasound and mechanical homogenization to enhance the stability of salad dressing emulsions containing acacia gum. The results showed that the mean size of the samples using power ultrasound and scaled-up homogenizer was 3.13 and 29.73 µm, respectively. Also, the energy consumption in the emulsification process of the samples treated with power ultrasound and scaled-up homogenizer was 26.4 and 330 J/mL emulsion, respectively.

Safe surfactants such as Tween 80 and Span 80, which are less toxic and highly compatible with other ingredients, can prepare nanoemulsions with stable droplet sizes. Span 80 is a lipophilic emulsifying agent, and Tween 80, a derivative of Span 80, has a hydrophilic nature with more solubility in water compared to oil. Tween 80 and Span 80 as nonionic surfactants with uncharged molecules are commonly noted as safe and biocompatible additives in food materials that are not influenced by pH variations. To produce nanoemulsions with proper stability, hydrophilic and lipophilic properties are balanced, and the combination of Span 80 and Tween 80 is usually applied (Shahavi et al., 2015, 2016). When using Tween 80 and Span 80 simultaneously, the significant difference in the headgroup size of Tween 80 and Span 80 enhances the synergistic effect between them, leading to increase the stability of nanoemulsions. Mixed surfactants also promote the stability of the nanoemulsions by strengthening the interfacial layer of the nanoemulsion systems. This might be due to the fact that mixed surfactants with hydrophilic and lipophilic properties favor adsorption between the oil and water phases (Chong et al., 2018).

The production of nanoemulsions containing EO and active compounds has been investigated using different methods in various studies. For example, Das et al. (2021) evaluated the antimicrobial, anti-aflatoxigenic, and antioxidant properties of chitosan nanoemulsion containing the *Anethum graveolens* EO using the ionic gelation technique compared to its EO. Chaudhari et al. (2020) evaluated the preservation capacity of the chitosan nanoemulsion to hinder the spoilage of stored corn against microbial contamination and lipid oxidation. They produced the nanoemulsion using the ionic gelation method by different ratios of chitosan, anethole, and tripolyphosphate as a crosslinking agent. Ghaderi-Ghahfarokhi et al. (2016) used thyme EON in the chitosan matrix to improve the antimicrobial and antioxidant properties of the EO. They prepared the EON using oil/water emulsion and ionic gelation. Tiwari et al. (2022) used chitosan containing *Cinnamomum glaucescens* EON as a new preservative to control food-borne fungi. The EON significantly improved the antifungal and anti-aflatoxin properties compared to the EO.

Since oxygenated monoterpenes present in the FSLB have significant antioxidant and antimicrobial properties (Mehrabanjoubani et al., 2021; Mirzania et al., 2019), this plant has the potential to be used in the food industry. Besides, the constituents of the FSLB's EO are diverse depending on the geographical region, different parts of the plant, and the time of harvesting (before or after flowering), leading to different properties (Mehrabanjoubani et al., 2021; Mirzania et al., 2019; Mohammadzadeh et al., 2018). To better understand the relationship between various characteristics of the EO with its constituents, it is necessary to identify the plant's composition based on its origin. Despite all the research done, there is limited information in the literature concerning the composition and antioxidant and antimicrobial properties of the EO of the FSLB (Mohammadzadeh et al., 2018; Morteza-Semnani et al., 2009; Rustaiyan et al., 2001). However, there is no study on the nanoemulsification of the FSLB's EO using ultrasound with food-grade emulsifiers and assessing its resultant properties during storage. Therefore, the aims of this research were as follows: (1) to identify the chemical composition of the EO of the FSLB; (2) to produce the EON by ultrasonication; (3) to evaluate the mean particle size, PDI, and zeta potential of the EON and blank nanoemulsion (BN) during a 60-day storage period; and (4) to compare the antioxidant and antimicrobial properties of the EO and EON.

Material and Methods

Materials

The FSLB was planted and grown in organic conditions at a garden located in Gaskar Mahalleh, Roudsar, Guilan province, Iran. The leaves of the FSLB were collected in June 2020 and dried at room temperature (25 °C) for 72 h. The leaves were identified in the herbarium of the Medicinal Plants and Drugs Research Institute, Shahid Beheshti University, Tehran, Iran. Microbial strains of *Escherichia coli* (ATCC 25922) and *Staphylococcus aureus* (ATCC 25923) were obtained from the Iranian Research Organization for Science and Technology (IROST). Additionally, methanol, Tween 80, Span 80, sodium nitroprusside, phosphate-buffered saline, sulfanilamide, *N*-(1-naphthyl) ethylenediamine dihydrochloride, phosphoric acid, *n*-hexane, 2,2-diphenyl-1-picrylhydrazyl (DPPH) (Sigma-Aldrich, USA), sodium sulfate, dimethyl sulfoxide (DMSO), Muller-Hinton agar, and Muller-Hinton broth (Merck, Germany) were used in this investigation.

Extraction of the FSLB's EO and Evaluation of Its Compounds

The EO of the FSLB was obtained by hydrodistillation extraction for 3 h using a Clevenger-type apparatus. Anhydrous sodium sulfate was used to dehydrate the EO and then filtered. It was then stored in the refrigerator at 4 °C in dark glass bottles until further analyses (Hasheminya & Dehghannya, 2020c).

The EO was analyzed using gas chromatography and mass spectrometry (GC-FID and GC–MS). GC-FID analyses were performed using a gas chromatograph (Agilent 7890A, Palo Alto, CA, USA), equipped with HP-5 ms capillary column (30 m × 0.25 mm i.d; film thickness 0.25 µm) and a flame ionization detector (FID). The temperature of the column was adjusted to 50 °C for 3 min. It was then raised to 240 °C at 3 °C/min and kept at this temperature for 9 min. The carrier gas was helium at 1.03 mL/min. Detector and injector temperatures were 260 and 202 °C, respectively. Besides, the split ratio was set to 1:50. Injected volume was 1 µL of the EO in *n*-hexane (10%).

A gas chromatograph (Model GC-17A, Version 3, Shimadzu, Japan) equipped with a column DB-5 (polydimethylsiloxane, dimensions 60 m × 0.25 mm and thin layer thickness of 0.25 µm) was connected to a mass spectrometer (Model QP-5050A, Shimadzu, Japan) (GC–MS) using an electron ionization device, EI, and a quadrupole analyzer (Agilent 5973) to identify the EO composition. The temperature program was the same used for GC-FID. The volume injected and the flow rate was 1 µL of the EO in *n*-hexane (10%) and 1.03 mL/min, respectively. MS transfer line temperature, EI ion source temperature, and quadrupole temperature were 230 °C, 200 °C, and 160 °C, respectively, with ionization energy of 70 eV.

Constituent identification was carried out by comparison of their retention indexes (RI) to a standard *n*-alkane series (C6-C40) as well as by a comparison of its mass spectrum with either reference data from the equipment database (NIST 21, NIST 107, NBS 75 K and WILEY229) or the literature (Hasheminya & Dehghannya, 2020c; Adams, 2007).

Essential Oil Content

The essential oil content obtained after extraction was calculated as the ratio of the mass of the essential oil to the dried leaves (Hasheminya & Dehghannya, 2020c):

$$\text{Essential oil content}(\%) = \frac{m_{EO}}{m_s} \times 100 \quad (1)$$

where m_{EO} and m_s represent the mass of EO (g) and dried leaves (g), respectively.

Essential Oil Nanoemulsion Preparation

To prepare the oil in water (O/W) nanoemulsion at ambient temperature, Tween 80 and Span 80 surfactants (10% w/w), the EO of the FSLB (10% w/w), and deionized water (80% w/w) were used with hydrophilic-lipophilic balance (HLB) of 12. The HLB value of the mixed surfactant system was calculated as follows (Shahavi et al., 2016):

$$\mathrm{HLB} = \frac{m_A \times \mathrm{HLB}_A + m_B \times \mathrm{HLB}_B}{m_A + m_B} \quad (2)$$

where m_A and m_B represent the mass of surfactant A (Tween 80) and surfactant B (Span 80), respectively. HLB_A and HLB_B stand for the HLB value of surfactants A and B, respectively.

Tween 80 with $HLB_A = 15.0$ and $m_A = 72\%$ and Span 80 with $HLB_B = 4.3$ and $m_B = 28\%$ were chosen for the nanoemulsion preparation. To obtain the HLB value, a series of initial experiments were carried out, and the HLB of 12 demonstrated the highest stability among all the samples tested. To prepare the aqueous phase, Tween 80 was added to the deionized water at ambient temperature, and the solution was stirred for 10 min. The oil phase was also prepared by adding Span 80 to the EO. The initial emulsion was prepared by adding the oil phase to the aqueous phase, drop by drop, homogenized by stirring. In the next step, the homogenization process continued by stirring for 15 min. Finally, the whole mixture (25 mL sample inside a 50-mL beaker) was treated using probe sonicator (Model UP400S, Hielscher GmbH, Germany) with a solid sonotrode H7 made of titanium with tip diameter of 7 mm and length of 100 mm at 400 W power, 24 kHz frequency, and 100% amplitude (100 µm) at ambient temperature (25 °C) for 20 min. In order to keep the temperature below 30 °C during ultrasonication, the nanoemulsions were maintained in an iced water bath (Gharenaghadeh et al., 2017; Nirmal et al., 2018; Shahavi et al., 2015). The method of producing EON is shown in Fig. 1.

Blank nanoemulsion (BN) was also prepared to evaluate and compare the properties of EO and EON. To prepare the BN, the same method for the preparation of EON was applied by replacing the essential oil with medium chain triglycerides (MCTs). Baldissera et al. (2013) and Santos et al. (2020) have also used the BN containing MCT to compare it with nanoemulsions containing essential oil.

Droplet Size Distribution, PDI, and Zeta Potential

Zetasizer Nano-ZS (Malvern instrument, Worcestershire, UK) was used to determine the mean particle size, polydispersity index (PDI), and zeta potential of samples on days 1, 15, 30, 45, and 60 at 25 °C. To avoid interactions between droplets, dispersion, and multiple scattering, deionized water (1: 100) was used as a dispersant (Hasheminya & Dehghannya, 2021).

SEM

The morphology (shape and size) of the freeze-dried EON and BN samples was evaluated by scanning electron microscope (Model MIRA3 FEG-SEM, Tescan, Czech Republic). The samples were imaged at 10 kV after being coated with gold (Hasheminya et al., 2019a).

XRD

X-ray diffraction patterns of the freeze-dried samples were obtained using an x-ray diffractometer (Model Kristalloflex D500, Siemens, Germany) with Cu Kα radiation at 42 kV,

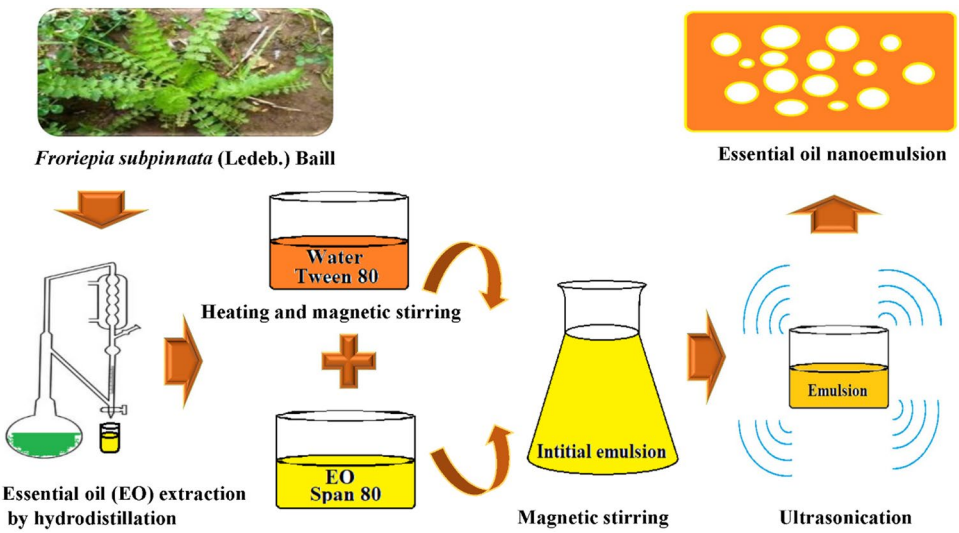

Fig. 1 Schematic diagram of *Froriepia subpinnata* (Ledeb.) *Baill* essential oil nanoemulsion (EON) production using ultrasound

the current intensity of 30 mA in the range of diffraction angles (2θ) from 0 to 60° (Hasheminya & Dehghannya, 2020a).

FTIR Spectroscopy

Fourier transform infrared (FTIR) spectroscopy (Model Tensor 27, Brucker, Germany) was used to determine functional groups of the EO, BN, and EON samples in the wavenumber range of 400–4000 cm^{-1} (Liu & Liu, 2020).

Antioxidant Activity by DPPH

The antioxidant capacity of the EO, BN, and EON was assessed on days 1, 15, 30, 45, and 60 at 25 °C by measuring the DPPH (2,2-diphenyl-1-picrylhydrazyl) activity. Fifty microliters of the sample was mixed at different concentrations (100, 50, 25, 12.5, and 6.25 µg/mL) with 2 mL of DPPH (60 µM) methanol solution. After mixing, the samples were shaken using a shaker incubator for 30 min and then stored in a dark room at 25 °C. Afterward, the sample absorbance intensity was recorded at 517 nm by a spectrophotometer. Butylated hydroxytoluene (BHT) antioxidant was considered as a positive control. The DPPH scavenging activity was calculated as follows (Hasheminya & Dehghannya, 2020c):

$$\text{DPPH scavenging activity}(\%) = \left(\frac{A_{DPPH} - A_S}{A_{DPPH}}\right) \times 100 \quad (3)$$

where A_{DPPH} is the absorbance of the DPPH solution without the sample, and A_S shows the absorbance of the DPPH solution with the sample. After measuring the percentage of DPPH free radical scavenging activity, the IC_{50} value was calculated. IC_{50} represents the concentration of the EON, which can inhibit 50% of free radicals.

Antioxidant Activity by Nitric Oxide

The antioxidant activity of the EO, BN, and EON was assessed on days 1, 15, 30, 45, and 60 at 25 °C based on nitric oxide free radicals scavenging activity. Sodium nitroprusside (10 mM) in phosphate-buffered saline was initially added to different concentrations of the samples (100, 50, 25, 12.5, and 6.25 µg/mL). The mixture was then incubated for 150 min at room temperature. Furthermore, 0.5 mL of Griess reagent (including 1% sulfanilamide, 1% *N*-(1-naphthyl) ethylenediamine dihydrochloride, and 2% phosphoric acid) was added to the mixture. The absorbance of the mixture was then read at 546 nm by the spectrophotometer. The following equation was used to calculate the percentage of nitric oxide radical scavenging activity (Sreejayan & Rao, 1996):

$$\text{NO scavenging activity}(\%) = \left(\frac{A_{NO} - A_S}{A_{NO}}\right) \times 100 \quad (4)$$

where A_{NO} shows the absorbance of the NO solution without the sample, and A_S expresses the absorbance of the NO solution with the sample. After measuring the percentage of nitric oxide radical scavenging activity, IC_{50} was calculated.

Antimicrobial Properties

The minimum inhibitory concentration (MIC) and the minimum microbicidal concentration (MMC) of the samples were determined by the microdilution method. To perform this test, 100 µL of different concentrations of the EO, BN, and EON on days 1, 15, 30, 45, and 60 at 25 °C, obtained by serial dilutions (160 to 0.312 mg/mL), was added to 90 µL Muller-Hinton Broth medium. Then, 10 µL of bacterial suspensions equivalent to 5×10^6 CFU/mL was added to the wells containing the medium and different sample dilutions. The samples were then incubated for 24 h at 37 °C. The lowest concentration in which no microorganism growth was noticed was determined as MIC. Streptomycin antibiotic was used as a positive control. The minimum microbicidal concentration was measured based on the MIC values. One hundred microliters of the contents of the wells in which the growth of microorganisms was halted was transferred to the Muller-Hinton Agar culture medium and incubated for 24 h at 37 °C. The lowest concentration of the EO and EON without microorganism growth was considered MMC (Hasheminya & Dehghannya, 2020c).

Statistical Analysis

Statistical analysis was executed on the measured characteristics, including the mean particle size, PDI, and zeta potential in the BN and EON, as well as the antioxidant and antimicrobial properties of the EO and EON at the same concentration (10%) in the form of completely randomized design (CRD). All the experiments were conducted in triplicate. Duncan's multiple range test was used to compare the means at a 5% probability level. Analysis of ANOVA was done using SAS (version 9.4).

Results and Discussion

Chemical Composition of the EO of the FSLB

The EO content was 0.4%. The chemical composition of the EO obtained from the FSLB's leaves is shown in Table 1. In total, 28 chemical compounds were identified, the most important of which were p-cymen-8-ol (22.83%), limonene (8.87%), terpinolene (8.86%), γ-terpinene (6.79%),

Table 1 Chemical composition of the essential oil extracted from leaves of *Froriepia subpinnata* (Ledeb.)

No	Compound	Peak area%**	RI*
1	Hexanal	1.00	801
2	*n*-hexanol	1.27	863
3	α-pinene	5.73	932
4	Sabinene	1.22	976
5	β-pinene	2.76	980
6	Myrcene	1.05	988
7	*cis*-dehydroxylinalool oxide	4.17	1006
8	δ-3-carene	2.68	1008
9	o-cymene	1.04	1022
10	Limonene	8.87	1024
11	β-phellandrene	1.39	1025
12	γ-terpinene	6.79	1054
13	*n*-octanol	1.70	1063
14	Terpinolene	8.86	1086
15	*p*-cymen-8-ol	22.83	1179
16	Citronellol	2.09	1223
17	Pulegone	3.19	1233
18	Neral	2.60	1235
19	Carvone	1.68	1239
20	Carvenone	5.98	1255
21	*trans*-carvone oxide	1.78	1273
22	Thymol	1.38	1289
23	Menthyl acetate	1.50	1294
24	Carvacrol	1.76	1298
25	β-cubebene	1.37	1387
26	β-selinene	1.09	1489
27	Germacrene A	1.17	1408
28	β-Cedrene	3.05	1411
	Classification of compounds		
	Oxygenated monoterpenes	54.54	
	Monoterpene hydrocarbon	31.53	
	Sesquiterpene hydrocarbon	3.47	
	oxygenated sesquiterpenes	3.05	
	Miscellaneous compounds	7.2	
	Total identified	99.79	

*RI, Retention indices calculated from retention times in relation to those of a series of C6-C40 n-alkanes on a DB-5 capillary column

**Peak areas were obtained from GC analysis

carvenone (5.98%), and α-pinene (5.73%). The main chemical compounds were oxygenated monoterpenes (54.54%), monoterpene hydrocarbons (31.53%), sesquiterpene hydrocarbons (3.47%), and oxygenated sesquiterpenes (3.05%). In a similar study (Rustaiyan et al., 2001), the main components of the EO of the FSLB's aerial parts were β-phellandrene (50.3%), sabinene (25.7%), β-pinene (4.5%), and γ-terpinene (3.3%). In another study (Morteza-Semnani et al., 2009), the main chemical compositions of the EO extracted from the aerial parts of the FSLB were *p*-cymen-8-ol (34.7%), terpinolene (12.5%), *p*-cymene (10.5%), phellandral, and neophytadiene (3.5%). Besides, Mohammadzadeh et al. (2018) reported that the main components of the EO obtained from the green leaves and stems of the FSLB were cuminol (42.05%) and phenol (28%) before flowering and sabinene (25.96%) and thymol (22.68%) after flowering.

The EO composition depends on different parameters, including geo-climatic or altitudinal variations, plant age, conditions of cultivation, geography, temperature, length of the day, time of harvest, the organ of the plant where

the EO is obtained, EO-making techniques, and climatic conditions. These parameters affect the biosynthesis of plant pathways and subsequently influence the amounts of main compounds, which leads to the development of various chemotypes (Hasheminya & Dehghannya, 2020c; Das et al., 2021).

Evaluation of Mean Particle Size, PDI, and Zeta Potential

Droplet Size Distribution

The droplet size distribution of the BN and EON on days 1, 15, 30, 45, and 60 is shown in Fig. 2a. In general, when the size of the particles is decreased, the nanoemulsion stability is significantly increased (Shahavi et al., 2015). Results showed that the mean particle size of the BN and EON on the 1st day was 67.18 and 84.32 nm, respectively, which was in the nanoscale range (Shahavi et al., 2016), resulting from the preparation method by ultrasonication as well as the use of Tween 80 with HLB of 15 and Span 80 with HLB of 4.3. The ultrasonication technique applied in the preparation of the BN and EON is based on the cavitation mechanism. Based on this mechanism, continuous mechanical depressions and compressions result in bubble collapse, which leads to enough energy to intensify the interfacial area of the droplets. Consequently, ultrasonication can produce smaller droplet sizes (Yukuyama et al., 2015). Besides, severe droplet disruptions are created by cavitational collapse during ultrasonication at or near the interface in which very fine emulsions are formed (Canselier et al., 2002). Similarly, Zhu et al. (2018) attributed the formation of small-sized nanoemulsions to the cavitation and turbulent forces created during the ultrasonic process. Moreover, the surfactant used in the preparation of the BN and EON causes smaller droplets to form (Yukuyama et al., 2015). Aggregation and creaming phenomena can be prevented by a diameter reduction of the droplets in nanoemulsions through surfactant addition (Mendes et al., 2018). Emulsifying molecules such as Tween 80 and Span 80 are adsorbed at the oil and water interface, and, therefore, interfacial tension is decreased, which facilitates the formation of smaller particle sizes (Mendes et al., 2018). Through decreasing interfacial tension at the interface of oil and water, the surfactants reduce the free energy which is needed for the nanoemulsion formation (Ghosh et al., 2013).

Figure 2 a illustrates that the mean particle size of the EON was higher than the BN, which was due to the loading

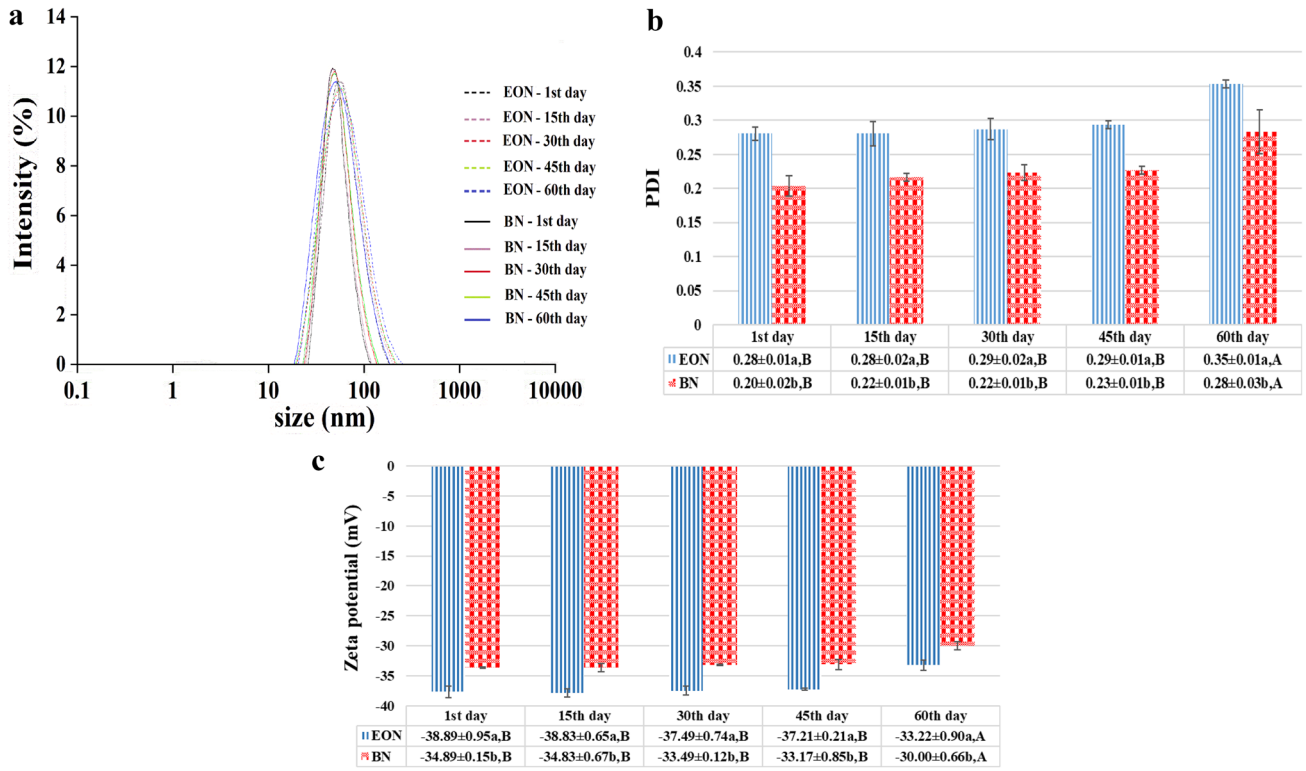

Fig. 2 Droplet size distribution (**a**), Polydispersity index (PDI) (**b**), and zeta potential (mV) (**c**) of *Froriepia subpinnata* (Ledeb.) Baill essential oil nonoemulsion (EON) and blank nonoemulsion (BN) on the 1st, 15th, 30th, 45th, and 60th days. *Different small letters in the columns indicate a significant difference ($p < 0.05$). **Different capital letters in the rows indicate a significant difference ($p < 0.05$)

of the EO. Similar findings were reported by Hosseini et al. (2013a) and Hosseini et al. (2013b). In addition, the results showed that the mean particle size of the BN and EON increased during storage from the 1st to the 45th days of storage; however, this increase was not statistically significant, indicating appropriate physical stability of the nanoparticles (Fig. 2a). This phenomenon can be ascribed to the dehydration of the surfactant head groups and consequent reduction of interfacial tension (Ziani et al., 2012). In similar research (Gharenaghadeh et al., 2017), stability of the *Salvia multicaulis*'s EON over 45 days of storage was noticed. This stability was attributed to Tween 80 and Span 80, which reduced the diffusion of the dispersed phase molecules through the continuous phase. Moreover, Moghimi et al. (2016) attributed the stability of the sage EON to the addition of Tween 80 and Span 80 surfactants and ultrasound treatment. Shahavi et al. (2015) also used Span 80 and Tween 80 surfactants to prepare the clove's EON by ultrasonication. They reported the size of the nanoemulsions at about 100 nm (Shahavi et al., 2015).

In contrast, the mean particle size of the BN and EON on the 60th day of storage was significantly higher than the previous samples (Fig. 2a). The size of droplets is slightly raised for long durations due to the interaction of the nanoemulsion molecules (Shahavi et al., 2015). Although the mean particle size increased over 60 days, it was always less than 100 nm during this period. An increase in the mean particle size of nanoemulsions during different storage periods was observed by Gharenaghadeh et al. (2017), Wang et al. (2021), and Ziani et al. (2012). Nanoemulsions, similar to emulsions, are semi-stable and change over time due to gravitational breakup, coalescence, and Ostwald ripening. Nanoemulsions are more stable than emulsions against gravitational separation and coalescence. However, due to their smaller particle size, they are more vulnerable to Ostwald ripening (Gharenaghadeh et al., 2017), which is, seemingly, the primary mechanism of the stability breakdown in the O/W nanoemulsions. The dispersed phase molecules from smaller to larger droplets are diffused through the continuous phase, enhancing the droplets' collisions, favoring the coalescence process. This leads to dissolving smaller droplets and growing larger ones, which influences the stability of the nanoemulsions in a more extended period (Lago et al., 2019; Wang et al., 2021; Yukuyama et al., 2015; Ziani et al., 2012). Based on the collision theory, droplets with small sizes collide, and, consequently, droplets with larger sizes are produced (Shahavi et al., 2015). Ostwald's ripening mechanism can be slowed down by applying emulsifiers and surfactants to generate a barrier at the droplets' interfaces (Yukuyama et al., 2015). Jiang et al. (2019) observed the smaller size of the droplets as an essential factor for emulsion stability. They stated that small emulsion droplets decrease the chances of the particles' sedimentation by reducing their aggregation. Overall, the mean particle size is affected by various variables, including the type and concentration of stabilizers and operational factors such as temperature, sonication, and homogenization parameters (Ziani et al., 2012).

PDI

PDI of the BN and EON on the 1st, 15th, 30th, 45th, and 60th days is shown in Fig. 2b. PDI is an essential physical property considered during the manufacturing of food or pharmaceutical products, due to its impact on characteristics such as product performance, processability, stability, and appearance of the end product (Wang et al., 2021; Ziani et al., 2012). Results showed that the PDI of the BN and EON was less than 0.5 during the whole 60-day storage (Fig. 2b). The PDI of nanoparticles is theoretically between 0 and 1, where the values greater than 0.5 represent a substantial dispersion of particles and values of less than 0.5 characterize a narrow distribution of nanoparticles (Tamjidi et al., 2013). The formation of smaller nanoparticles and the PDI values between 0.2 and 0.35 for the BN and EON confirmed the effectiveness of the ultrasonic process in the production of a nanoemulsion with uniform distribution of its particle sizes (Noori et al., 2018).

The PDI of the BN and EON on the 1st day was 0.20 and 0.28, respectively (Fig. 2b). The higher PDI of the EON compared to the BN was due to the presence of essential oil in the EON. This result was consistent with Bazana et al. (2019) and Hosseini et al. (2013b). The results also showed that the PDI of the BN and EON on the 45th day was not significantly different from the samples of the 1st, 15th, and 30th days. However, the PDI of the BN and EON on day 60 was significantly different from days 1, 15, 30, and 45. Parameters such as oil type, storage temperature, oil concentration, and incubation time affect colloidal dispersions during the storage period (Ziani et al., 2012).

Zeta Potential

Zeta potential represents the particles' net charge and is an essential indicator for evaluating the stability of nanoemulsions during storage (Hasheminya & Dehghannya, 2021). Zeta potential of the BN and EON on the 1st, 15th, 30th, 45th, and 60th days is shown in Fig. 2c. The zeta potential of the BN and EON was in the range of −30 to −38.89 mV during the 60 days (Shahavi et al., 2016). Stable particles possess a zeta potential of above + 30 mV and below −30 mV (Salvia-Trujillo et al., 2013). A high surface charge due to electrostatic repulsion between particles with the same electric charge reduces the risk of coagulation, making the system more durable for a long time (Shahavi et al., 2016). The surfactants' charge attached around oil droplets determines

the electrical charge of emulsion droplets (Hasheminya & Dehghannya, 2021). In addition to the nature of the constituents of the nanoemulsions that leads to the formation of specific zeta potentials, when they are subjected to severe mechanical stresses such as ultrasound, free hydroxyl and carboxyl groups are likely to release from the components of the systems and move to the surface of the droplets and expose to water. These changes lead to a change in the zeta potential of the nanoemulsions. Deprotonated alcohols and carboxylic acids enhance the nanoemulsions' negative charge throughout ultrasonic treatment (Hasheminya & Dehghannya, 2021).

The results also showed that adding the essential oil increased the zeta potential (Fig. 2c). These results were similar to those of Bazana et al. (2019). The ionizable molecules in the constituents of the EO lead to the higher negative zeta potential of the EON (Hasheminya & Dehghannya, 2021). In addition, the results showed that with the increase of the storage period up to 45 days, the zeta potential for the BN and EON decreased, but this decrease was not significant. In other words, the zeta potential of the BN and EON samples on the 45th day of storage was not significantly different from the samples of the 1st, 15th, and 30th days. Negative values less than −30 and no significant change of zeta potential for the BN and EON during 45 days (Fig. 2c) indicated the stability of nanoemulsions (Salvia-Trujillo et al., 2013). However, the zeta potential of the BN and EON on day 60 was significantly reduced compared to all the previous samples. Despite the significant difference in the zeta potential of the BN and EON on the 60th day compared to the previous days, zeta potential values less than −30 pointed to the stability of the nanoemulsions (Salvia-Trujillo et al., 2013). These results were similar to those of Li et al. (2020), which could be ascribed to chemical hydrolysis of the surfactants at more extended storage periods, causing to lose its ability in the formation of micelles and emulsion stabilization (Ziani et al., 2012).

SEM

Figure 3 illustrates the microstructure of the BN and EON obtained from SEM. As shown in the figure, semispherical BN and EON were produced without aggregation, which indicated the stability of the particles during the nanoemulsion preparation process (Gharenaghadeh et al., 2017; Hosseini et al., 2013a). The proper distribution of EON droplets in the aqueous phase can be due to the formation of micelles with semispherical structure. Surfactants reduce the interfacial energy between oil and water systems by forming a layer around dispersed oil droplets, leading to form nanoemulsions by preventing particles from coalescence (Safaya & Rotliwala, 2022). SEM images showed that the BN and EON were almost identical. The particle size of both BN and EON acquired from the SEM images (less than 100 nm) confirmed the Zetasizer results.

X-Ray Diffraction

Figure 4 illustrates the XRD pattern of the EO, BN, and EON samples. A band at the 2θ = 20 was noticed in the BN and EON, which indicated the predominant amorphous nature of these samples with very low crystallization. However, the XRD pattern of the EO almost illustrated the whole amorphous nature of the essential oil. This finding was in line with Hasheminya et al. (2019b), Chaudhari et al. (2020), and Das et al. (2021). After adding the essential oil, the peak intensity of the EON was reduced compared to the BN (Fig. 4). This phenomenon can be attributed to the reduction in crystallinity of the EON and the homogeneous distribution of the essential oil in the nanoemulsion matrix (Galvao et al., 2020). The formation of a weaker crystal structure is a crucial factor in increasing the entrapment of active substances such as essential oils in the nanoemulsion network (Bhalekar et al., 2009). Chaudhari et al. (2020) also considered the change in the arrangement form of molecules in the structure of the matrix network due to the influence of additives as the cause of variations in the XRD pattern. Furthermore, Das et al. (2021) observed destruction in crystallinity of chitosan powder containing the *Anethum graveolens* EON. They attributed this behavior to the electrostatic interactions between chitosan, sodium tripolyphosphate, and the active components of the EO.

FTIR

Figure 5 illustrates the FTIR spectra for EO, BN, and EON. For EO, the characteristic peaks at 3700–3100 cm^{-1} corresponded to the OH stretching (Hasheminya et al., 2019a). The spectra showed characteristic bands at 2962 and 2869 cm^{-1} (CH stretching), 2728 cm^{-1} (stretching aldehyde; C = O), 1860 cm^{-1} (carbonyl anhydride), 1731 and 1710 cm^{-1} (C = O stretching), 1635 cm^{-1} (vibration for $RHC=CH_2$), 1580 cm^{-1} (C–O–C stretching vibration of CH_3), 1520 cm^{-1} (CH (CH_3)), 1446 cm^{-1} (C = C bending), 1375 cm^{-1} (isopropyl group), 1237 cm^{-1} (C–O–C and C–OH bonds), 1174 cm^{-1} (C = C), and 1132 cm^{-1} (C–O–C stretching) (Shetta et al., 2019). The peaks at 973 and 937 cm^{-1} were assigned to the C–H bending vibration (Hosseini et al., 2013a; Li et al., 2013). The band at 875 cm^{-1} was attributed to the α-pinene for strained ring structures with an exocyclic $=CH_2$ group, and the peak at 805 cm^{-1} was related to the HC = CH– (cis–) bending (Sadowska et al., 2019). The spectrum also demonstrated the peaks at 722 cm^{-1} (CH_2 and cis –HC = CH – vibrations), 685 cm^{-1} (vibration of alkenes), and 570 cm^{-1} (aromatic ring vibration) (Li et al., 2013).

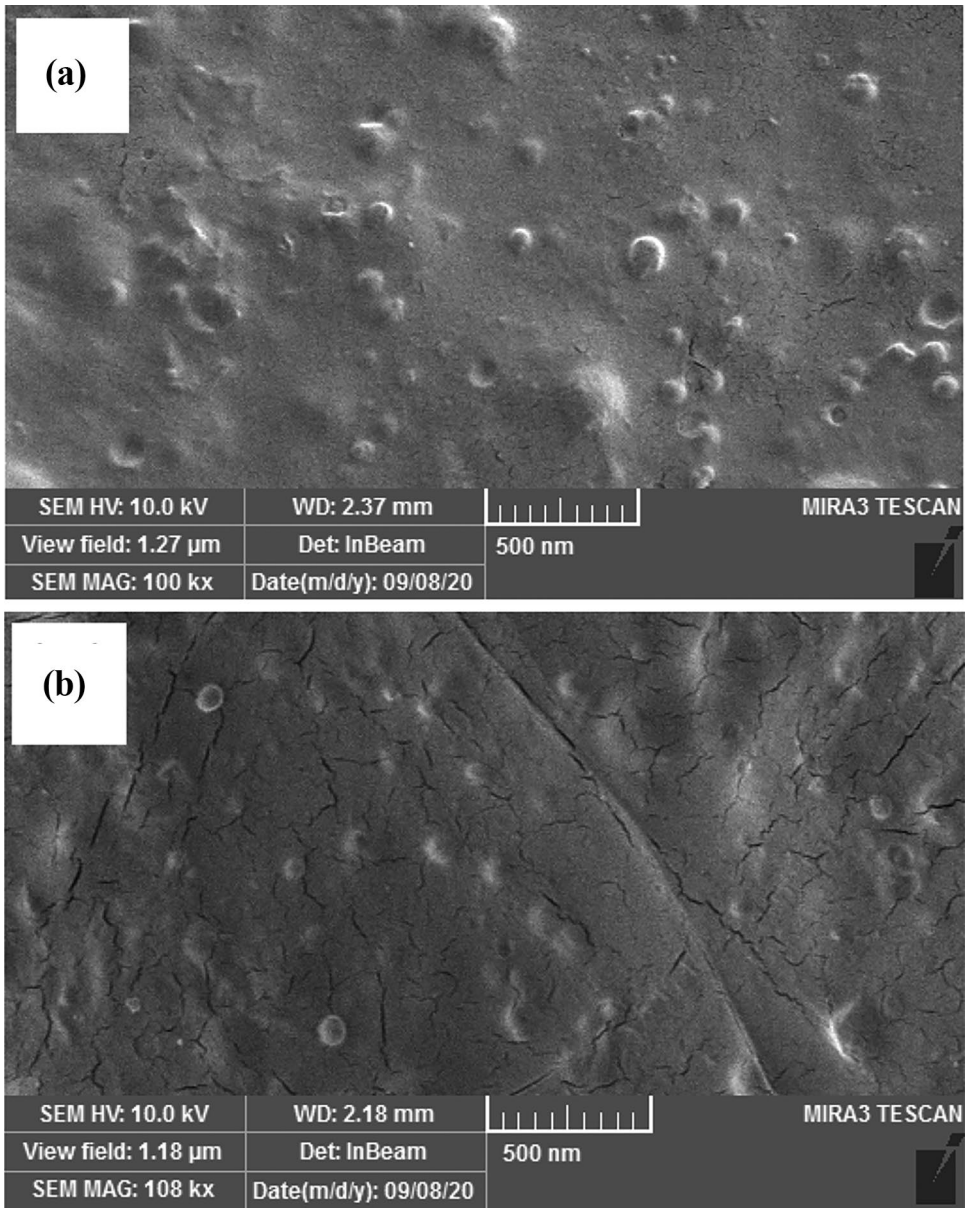

Fig. 3 Scanning electron microscopy (SEM) images of *Froriepia subpinnata* (Ledeb.) *Baill* essential oil nanoemulsion (EON) (**a**) and blank-nanoemulsion (BN) (**b**)

The BN showed several specific absorption bands (Fig. 5). The peaks ranging at 3000–3600 cm^{-1} in the spectrum were attributed to the free OH groups (Hosseinnia et al., 2013). Also, the bands at the 3000–2800 cm^{-1} were linked to the C–H stretching vibrations (Hasheminya et al., 2018). The peak at 1740 cm^{-1} was associated with the C–C bands (Liu & Liu, 2020). The spectrum also illustrated the peaks at 1648 cm^{-1} (–C = C–, cis–), 1520 cm^{-1} (CH (CH_3)), and 1458 cm^{-1} (–C–H, cis– bending) (Sadowska et al., 2019).

The spectrum of the EON showed a slight change compared to the BN (Fig. 5). The intensity of the 2927 and 2869 cm^{-1} peaks in the EON increased compared to the BN, indicating an increase in the content of ester groups linked to the EO molecules. Similar findings were observed by Hosseini et al. (2013a), Hosseini et al. (2013b), and Liu and Liu (2020). Although the peaks at 1132 and 875 cm^{-1}, which presented in the EO, were also observed in the EON, the other peaks in the EO were not observed in the EON. Similar findings were noticed by Banerjee et al. (2013), Hosseini et al. (2013a), and Hosseini et al. (2013b). Observing some of the peaks of *Zanthoxylum limonella* essential oil in the spectrum of carbohydrate polymer-protein blends, Banerjee et al. (2013) concluded that the presence of essential oil in the polymer matrix was stable and that no chemical interaction between the essential oil and the matrix composition took place. In another study, by observing some peaks related to the essential oil of *Satureja hortensis* in an alginate matrix, Hosseini et al. (2013b) observed the presence of essential oil particles in the nanoemulsion. The disappearance of some peaks related to the active substance

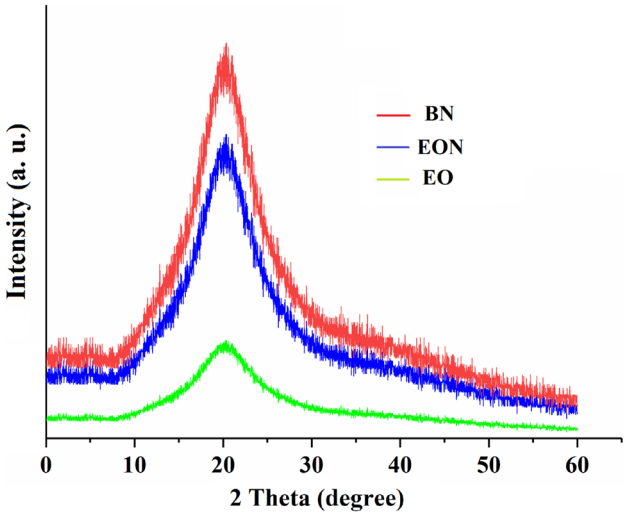

Fig. 4 XRD patterns for the essential oil of *Froriepia subpinnata* (Ledeb.) *Baill* (EO), *Froriepia subpinnata* (Ledeb.) *Baill* essential oil nanoemulsion (EON), and blank-nanoemulsion (BN)

(EO) in the spectrum of the nanoemulsion (EON) in our study has been observed in some other investigations (Fan et al., 2014; Gharenaghadeh et al., 2017). This phenomenon can signify the essential oil entrapment inside the lipid (surfactant) matrix during the formation of nanoemulsions (Fan et al., 2014). In addition, the displacement of the hydroxyl group in the EO (3438 cm^{-1}) to lower wavenumber (3427 cm^{-1}) in the EON indicated the formation of hydrogen bonds between the constituents of the EO and the surfactants used (Hasheminya et al., 2018).

Antioxidant Activity

The IC_{50} values obtained from the DPPH free radicals scavenging activity for the EO, EON, and BHT were, respectively, 487.23, 388.65, and 22.35 µg/mL on the 1st day (Table 2). This result showed that both the EO and EON had antioxidant activity. Besides, IC_{50} values obtained from nitric oxide free radicals scavenging activity for the EO, EON, and BHT were 384.65, 309.62, and 16.15 µg/mL, respectively, on the 1st day (Table 2). In other words, the antioxidant activity of the EON was higher compared to the EO in both the measurement methods (The smaller the IC_{50} values, the stronger the antioxidant properties). Similar findings were observed by Babaoglu et al. (2017), Das et al. (2021), Gharenaghadeh et al. (2017), Lou et al. (2017), Manea et al. (2013), and Tiwari et al. (2022).

Since the EO is not dissolved in aqueous systems, this can reduce the antioxidant activity of the EO. However, the EON with good solubility in aqueous systems is suitable for the effective delivery of active compounds. Due to a larger surface area, quick diffusion of active ingredients is

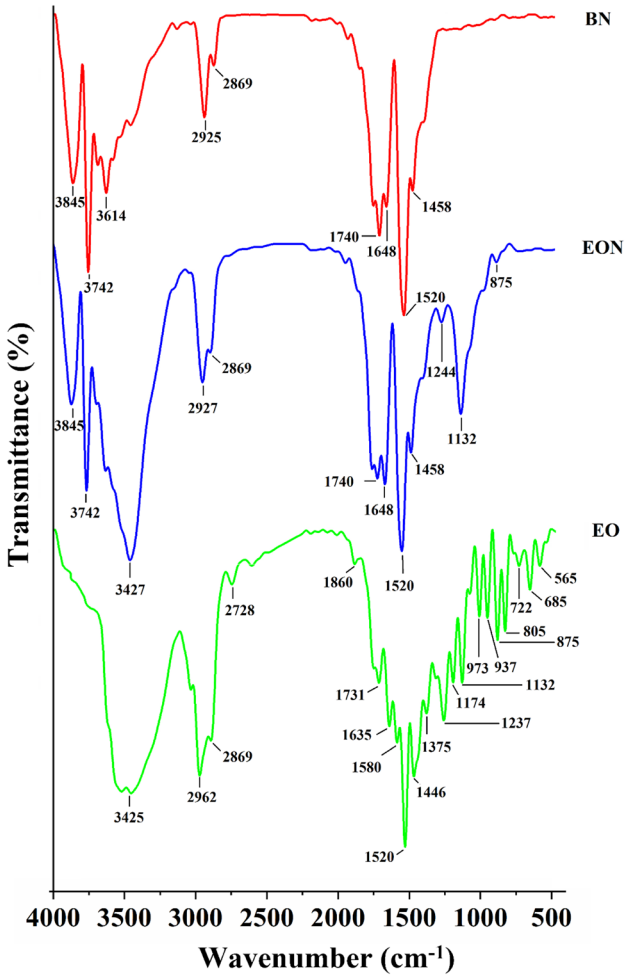

Fig. 5 Fourier transform infrared (FTIR) spectroscopy for the essential oil of *Froriepia subpinnata* (Ledeb.) *Baill* (EO), *Froriepia subpinnata* (Ledeb.) *Baill* essential oil nanoemulsion (EON), and blank-nanoemulsion (BN)

achieved. Consequently, the EON can hinder free radicals more effectively, demonstrating further antioxidant activity (Lou et al., 2017). Also, droplet size reduction due to the nanoemulsion formation leads to increasing the specific surface of the essential oil, thus achieving an efficient free radical scavenging activity (Noori et al., 2018).

In a similar study, Babaoglu et al. (2017) showed that nanoemulsification of the clove's EO in hydroxypropyl beta-cyclodextrin improved the antioxidant activity of the EON compared to the EO. The increased antioxidant activity was ascribed to enhancing the EON's water solubility due to the nanoemulsification. Besides, Manea et al. (2013) noticed an improvement in the antioxidant properties of green tea extract loaded into nanostructured lipid carriers compared to the green tea extract and attributed this phenomenon to the mean particle size, the nanoemulsifying effect, and the synergy between the complex lipid matrixes. Bazana et al.

Table 2 Antioxidant activity of the *Froriepia subpinnata* (Ledeb.) *Baill* essential oil (EO), *Froriepia subpinnata* (Ledeb.) *Baill* essential oil nanoemulsion (EON), and BHT by DPPH and nitric oxide (NO) free radicals scavenging activity (IC_{50}; µg/mL) on the 1st, 15th, 30th, 45th, and 60th days of storage

Method	Samples	1st day	15th day	30th day	45th day	60th day
DPPH	EO	487.23 ± 0.05a,D	488.69 ± 0.12a,D	503.60 ± 1.12a,C	513.78 ± 2.00a,B	526.11 ± 1.15a,A
	EON	388.65 ± 0.37b,C	389.28 ± 1.76b,C	390.18 ± 0.07b,C	391.03 ± 0.12b,B	434.64 ± 0.38b,A
	BHT	22.35 ± 0.12c,A	22.04 ± 0.019c,A	22.15 ± 0.10c,A	22.75 ± 0.13c,A	21.32 ± 0.26c,A
NO	EO	384.65 ± 0.05a,D	384.65 ± 0.05a,D	418.37 ± 0.01a,C	418.37 ± 0.01a,B	418.37 ± 0.01a,A
	EON	309.62 ± 0.24b,C	310.48 ± 0.17b,C	310.90 ± 0.82b,C	311.02 ± 0.05b,B	362.48 ± 1.00b,A
	BHT	16.15 ± 0.27c,A	16.21 ± 0.15c,A	16.05 ± 0.30c,A	16.32 ± 0.11c,A	16.34 ± 0.05c,A

*Different lowercase letters in the same column for each method indicate a significant difference ($p < 0.05$)

**Different uppercase letters in the same row indicate a significant difference ($p < 0.05$)

(2019) also noticed antioxidant activity enhancement of the nanoemulsions containing the *Physalis peruviana* calyx extract compared to the extract, attributing this phenomenon to the protective effect of the nanostructured systems, which protect the bioactive compounds in the extract, resulting in the longer shelf life of the nano-capsulated extracts. Moreover, Das et al. (2021) attributed the increased antioxidant activity of nanoemulsions containing *Anethum graveolens* EO to the controlled release of EO from chitosan nanomatrix at higher surface-to-volume ratios. The formation of hydrogen bonds between hydroxyl groups in phenolic compounds and the chitosan matrix, which causes a controlled release of extract, can also increase antioxidant capacity.

In addition to the above, the results showed that the antioxidant activity of the EO and EON in both tested methods decreased over time (Table 2). The antioxidant activity of the EO was significantly reduced from the 30th day of storage compared to the 1st and 15th days. However, the antioxidant power of the EON decreased significantly from the 45th day of storage compared to the 1st, 15th, and 30th days. The gradual decrease in the antioxidant activity of the EON compared to the EO could be ascribed to the protective effect of the nanoemulsion (Bazana et al., 2019). These findings were in line with Bazana et al. (2019) and Noori et al. (2018). The physical and chemical instability of essential oils' phenolic compounds and their degradation due to external parameters such as oxygen, light, humidity, temperature, and pH are crucial factors in reducing the antioxidant power of the EO and EON (Bazana et al., 2019; Noori et al., 2018).

Antimicrobial Properties

The antimicrobial activities of the EO and EON are shown in Table 3. The EO and EON showed antimicrobial effects

Table 3 Minimum inhibitory concentration (MIC; mg/mL) and minimum microbicidal concentration (MMC; mg/mL) of the *Froriepia subpinnata* (Ledeb.) *Baill* essential oil (EO), *Froriepia subpinnata* (Ledeb.) *Baill* essential oil nanoemulsion (EON), and positive control (Gentamicin antibiotic) for *Escherichia coli* and *Staphylococcus aureus* on the 1st, 15th, 30th, 45th, and 60th days of storage

	Bacterium	Samples	1st day	15th day	30th day	45th day	60th day
MIC	*Escherichia coli*	EO	0.63 ± 0.00a,B	0.63 ± 0.00a,B	0.63 ± 0.00a,B	0.63 ± 0.00a,B	1.25 ± 0.00a,A
		EON	0.31 ± 0.00b,A	0.31 ± 0.00b,A	0.31 ± 0.00b,A	0.31 ± 0.00b,A	0.31 ± 0.00b,A
		Gentamicin	0.004 ± 0.00c,A	0.004 ± 0.00c,A	0.004 ± 0.00c,A	0.004 ± 0.00c,A	0.004 ± 0.00c,A
	Staphylococcus aureus	EO	0.31 ± 0.00a,B	0.31 ± 0.00a,B	0.31 ± 0.00a,B	0.31 ± 0.00a,B	0.63 ± 0.00a,A
		EON	0.16 ± 0.00b,A	0.16 ± 0.00b,A	0.16 ± 0.00b,A	0.16 ± 0.00b,A	0.16 ± 0.00b,A
		Gentamicin	0.004 ± 0.00c,A	0.004 ± 0.00c,A	0.004 ± 0.00c,A	0.004 ± 0.00c,A	0.004 ± 0.00c,A
MMC	*Escherichia coli*	EO	5 ± 0.00a,B	5 ± 0.00a,B	5 ± 0.00a,B	5 ± 0.00a,B	10 ± 0.00a,A
		EON	2.5 ± 0.00b,A	2.5 ± 0.00b,A	2.5 ± 0.00b,A	2.5 ± 0.00b,A	2.5 ± 0.00b,A
		Gentamicin	0.009 ± 0.00c,A	0.009 ± 0.00c,A	0.009 ± 0.00c,A	0.009 ± 0.00c,A	0.009 ± 0.00c,A
	Staphylococcus aureus	EO	1.25 ± 0.00a,B	1.25 ± 0.00a,B	1.25 ± 0.00a,B	1.25 ± 0.00a,B	2.5 ± 0.00a,A
		EON	0.63 ± 0.00b,B	0.63 ± 0.00b,B	0.63 ± 0.00b,B	0.63 ± 0.00b,B	0.63 ± 0.00b,B
		Gentamicin	0.009 ± 0.00c,A	0.009 ± 0.00c,A	0.009 ± 0.00c,A	0.009 ± 0.00c,A	0.009 ± 0.00c,A

*Different lowercase letters in the same column for each bacterium indicate a significant difference ($p < 0.05$)

**Different uppercase letters in the same row indicate a significant difference ($p < 0.05$)

against *Staphylococcus aureus* and *Escherichia coli*. The MIC of the EO varied from 0.63 mg/mL (*Staphylococcus aureus*) to 0.31 mg/mL (*Escherichia coli*) on the 1st day (Table 3). The MIC of the EON was from 0.16 mg/mL (*Staphylococcus aureus*) to 0.31 mg/mL (*Escherichia coli*) on the 1st day (Table 3). Besides, the MMC of the EO varied between 1.25 mg/mL (*Staphylococcus aureus*) and 5 mg/mL (*Escherichia coli*) (Table 3) on the 1st day. The MMC of the EON was between 0.63 mg/mL (*Staphylococcus aureus*) and 2.5 mg/mL (*Escherichia coli*) on the 1st day (Table 3). In general, the MIC and MMC of the EON were significantly below the EO in the tested bacteria, demonstrating a higher antimicrobial activity of the EON. Similar findings were observed by Gharenaghadeh et al. (2017), Jemaa et al. (2018), and Moghimi et al. (2016). The positive control (Gentamicin) in all the cases had a more substantial antibacterial effect than the EO and EON (Table 3).

Studies on the antimicrobial effect of the EO of the FSLB are scarce (Mohammadzadeh et al., 2018). Antibacterial characteristic of the EO is linked to their active constituents (including isoprenes such as monoterpenes and sesquiterpenes) and the hydrophobic property of their hydrocarbon structure with functional compounds (Hasheminya & Dehghannya, 2020c). Moreover, research has shown that compounds such as p-cymen-8-ol and limonene, identified in the EO, have also demonstrated antibacterial properties (Pires et al., 2006).

As noted, the antibacterial activity of the EON was better than the EO. The antimicrobial characterization of the nanoemulsions is attributed to their small particle sizes. Such droplets cause a quick fusion with bacterial cells and endanger their life (Jemaa et al., 2018). Besides, increasing the antibacterial properties of the EON is associated with enhancing its capacity to interrupt the cell membrane of bacteria (Moghimi et al., 2016). Sugumar et al. (2014) stated that the reduction in particle size by an ultrasonic process with increasing surface area leads to more significant interaction of nanoemulsion particles with bacterial membrane, causing to increase the antibacterial activity. Ghaderi-Ghahfarokhi et al. (2016) stated that emulsification of thyme EO in chitosan nanoparticles resulted in a better inhibitory effect on the Enterobacteriaceae family compared to the EO, indicating the synergistic effects of the EO and chitosan nanoparticles in controlling the gram-negative bacteria. Sepahvand et al. (2021) also noted that the antibacterial activity of the thymol EON was considerably higher than its EO against *Escherichia coli*, *Staphylococcus aureus*, and *Clostridium perfringens*. Uniform distribution of the EON in bacterial broth medium resulted in better performance than the EO. The oily nature of the EO caused a considerable amount of it to accumulate on the medium's surface, preventing its proper distribution in the medium, which ultimately led to a decrease in the performance of the EO.

In general, nanoencapsulation of EO in emulsifying systems increases their antimicrobial properties in three ways: (1) These systems can transfer the antimicrobial compounds to the layer of the cell membrane, in which case the compounds can be inserted into the membrane and affect the membrane from inside. (2) These systems act as carrier agents and bring specified concentrations of the compounds to the microorganisms within the aqueous phase. (3) At the surface of the bacterial membrane, some holes are the place of entry and exit of different compounds; the smaller the produced nanoemulsions, the more conveniently they can enter these holes and release their bioactive compounds (Gharenaghadeh et al., 2017).

Moreover, the results indicated that the antibacterial effect of both the EO and EON was higher on gram-positive (*Staphylococcus aureus*) bacteria than gram-negative (*Escherichia coli*) ones (Table 3). The enhanced vulnerability of the gram-positive bacteria is attributed to the absence of a lipopolysaccharide cell wall. This might hinder active compounds from crossing the membrane in the germ-negative bacterial cell wall. In general, antimicrobial mechanisms against different bacteria are rooted in their cell structure (Hasheminya et al., 2018). The outer membrane of the gram-negative bacteria restricts the release of lipophilic material through the lipopolysaccharide covering layer. In the gram-positive bacteria, direct contact of the hydrophobic constituents of the EO occurs with a two-layer phospholipid, which is where these active compounds generate their antimicrobial influence. This effect occurs either through enhancing ion diffusivity, dripping vital intracellular compositions, or damaging the bacterial enzyme system (Sandri et al., 2007).

Furthermore, the results showed that the MIC and MMC of the EO increased significantly on the 60th day of storage compared to the 1st, 15th, 30th, and 45th days; this is while the MIC and MMC of the EON did not change during the 60-day storage (Table 3). Similar observations have been noticed by Moraes-Lovison et al. (2017). The EON enhanced the antibacterial ability compared to the EO during the long-term storage by increasing the protection and stability of the bioactive compounds (essential oil). This phenomenon is critical for protecting food materials and enhancing their shelf life (Bazana et al., 2019; Moraes-Lovison et al., 2017).

Conclusions

The GC-FID and GC–MS analysis showed that the EO extracted from the leaves of the FSLB were composed of 28 compounds, the main of which was p-cymen-8-ol (22.83%). The results showed that the EON, produced using Tween 80 and Span 80 surfactants, and the ultrasonic process, was in the nano-scale range. Mean particle size, PDI, and zeta

potential of the EON did not change significantly during the 45-day storage, confirming its stability during this period. Spherical nanoparticles with a size of less than 100 nm were identified by SEM. Moreover, XRD and FTIR spectroscopy confirmed the essential oil nanoencapsulation. Antioxidant and antibacterial evaluations indicated that nanoencapsulation of the essential oil was able to improve and maintain these properties over time compared to the EO. The nanoemulsification method provided a convenient and effective way to enhance the activity and efficiency of the liposoluble active compounds. In conclusion, the present study showed that the FSLB's EO and its novel nanoemulsified form, developed using ultrasound and two surfactants, can be used as natural antioxidant and antimicrobial agents in related industries.

Funding This research was supported by a research grant from the University of Tabriz (Number: 3499).

Data Availability All data generated or analyzed during this study are included in this manuscript.

Declarations

Conflict of Interest The authors declare no competing interests.

References

Adams, R. P. (2007). *Identification of essential oil components by gas chromatography/mass spectrometry* (4th ed.). Allured Publishing Corporation.

Babaoglu, H. C., Bayrak, A., Ozdemir, N., & Ozgun, N. (2017). Encapsulation of clove essential oil in hydroxypropyl beta-cyclodextrin for characterization, controlled release, and antioxidant activity. *Journal of Food Processing and Preservation, 41*(5), e13202.

Baldissera, M. D., Silva, A. S. D., Oliveira, C. B., Zimmermann, C. E. P., Vaucher, R. A., Santos, R. C. V., Rech, V. C., Tonin, A. A., Giongo, J. L., Mattos, C. B., Koester, L., Santurio, J. M., & Monteiro, S. G. (2013). Trypanocidal activity of the essential oils in their conventional and nanoemulsion forms: In vitro tests. *Experimental Parasitology, 134*(3), 356–361.

Banerjee, S., Chattopadhyay, P., Ghosh, A., Goyary, D., Karmakar, S., & Veer, V. (2013). Influence of process variables on essential oil microcapsule properties by carbohydrate polymer–protein blends. *Carbohydrate Polymers, 93*, 691–697.

Bazana, M. T., Silva, SSd., Codevilla, C. F., Deus, Cd., Lucas, B. N., Ugalde, G. A., Mazutti, M. A., Flores, E. M. M., Barin, J. S., Silva, CdBd., & Menezes, CRd. (2019). Development of nanoemulsions containing *Physalis peruviana* calyx extract: A study on stability and antioxidant capacity. *Food Research International, 125*, 108645.

Bhalekar, M. R., Pokharkar, V., Madgulkar, A., & Patil, N. (2009). Preparation and evaluation of miconazole nitrate-loaded solid lipid nanoparticles for topical delivery. *Journal of the American Association of Pharmaceutical Scientists, 10*(1), 289–296.

Canselier, J. P., Delmas, H., Wilhelm, A. M., & Abismaïl, B. (2002). Ultrasound emulsification-an overview. *Journal of Dispersion Science and Technology, 23*(1–3), 333–349.

Chaudhari, A. K., Singh, V. K., Das, S., Deepika, S. B. K., & Dubey, N. K. (2020). Antimicrobial, aflatoxin B_1 inhibitory and lipid oxidation suppressing potential of anethole-based chitosan nanoemulsion as novel preservative for protection of stored maize. *Food and Bioprocess Technology, 13*, 1462–1477.

Chong, W.-T., Tan, C.-P., Cheah, Y.-K., Lajis, A. F. B., Dian, N. L. H. M., Kanagaratnam, S., & Lai, O.-M. (2018). Optimization of process parameters in preparation of tocotrienol-rich red palm oil-based nanoemulsion stabilized by Tween80- Span 80 using response surface methodology. *PLoS ONE, 13*(8), e0202771.

Das, S., Singh, V. K., Dwivedy, A. K., Chaudhari, A. K., & Dubey, N. K. (2021). *Anethum graveolens* essential oil encapsulation in chitosan nanomatrix: Investigations on in vitro release behavior, organoleptic attributes, and efficacy as potential delivery vehicles against biodeterioration of rice (*Oryza sativa* L.). *Food and Bioprocess Technology, 14*, 831–853.

Ezhilarasi, P. N., Karthik, P., Chhanwal, N., & Anandharamakrishnan, C. (2013). Nanoencapsulation techniques for food bioactive components: A review. *Food and Bioprocess Technology, 6*(3), 628–647.

Fan, H., Liu, G., Huang, Y., Li, Y., & Xia, Q. (2014). Development of a nanostructured lipid carrier formulation for increasing photostability and water solubility of phenylethyl resorcinol. *Applied Surface Science, 288*, 193–200.

Galvao, J. G., Santos, R. L., Silva, A. R. S. T., Santos, J. S., Costa, A. M. B., Chandasana, H., Andrade-Neto, V. V., Torres-Santos, E. C., Lira, A. A. M., Dolabella, S., Scher, R., Kima, P. E., Derendorf, H., & Nunes, R. S. (2020). Carvacrol loaded nanostructured lipid carriers as a promising parenteral formulation for leishmaniasis treatment. *European Journal of Pharmaceutical Sciences, 150*, 105335.

Gavahian, M., Chen, Y.-M., Khaneghah, A. M., Barba, F. J., & Yang, B. B. (2018). In-pack sonication technique for edible emulsions: Understanding the impact of acacia gum and lecithin emulsifiers and ultrasound homogenization on salad dressing emulsions stability. *Food Hydrocolloids, 83*, 79–87.

Ghaderi-Ghahfarokhi, M., Barzegar, M., Sahari, M. A., & Azizi, M. H. (2016). Nanoencapsulation approach to improve antimicrobial and antioxidant activity of thyme essential oil in beef burgers during refrigerated storage. *Food and Bioprocess Technology, 9*, 1187–1201.

Gharenaghadeh, S., Karimi, N., Forghani, S., Nourazarian, M., Gharehnaghadeh, S., Jabbari, V., & khiabani MS & Kafil HS,. (2017). Application of *salvia multicaulis* essential oil containing nanoemulsion against food-borne pathogens. *Food Bioscience, 19*, 128–133.

Ghosh, V., Saranya, S., Mukherjee, A., & Chandrasekaran, N. (2013). Cinnamon oil nanoemulsion formulation by ultrasonic emulsification: Investigation of its bactericidal activity. *Journal of Nanoscience and Nanotechnology, 13*(1), 114–122.

Hasheminya, S.-M., & Dehghannya, J. (2020a). Green synthesis and characterization of copper nanoparticles using Eryngium caucasicum Trautv aqueous extracts and its antioxidant and antimicrobial properties. *Particulate Science and Technology, 38*(8), 1019–1026.

Hasheminya, S.-M., & Dehghannya, J. (2020b). Novel ultrasound-assisted extraction of kefiran biomaterial, a prebiotic exopolysaccharide, and investigation of its physicochemical, antioxidant and antimicrobial properties. *Materials Chemistry and Physics, 243*, 122645.

Hasheminya, S.-M., & Dehghannya, J. (2020c). Composition, phenolic content, antioxidant and antimicrobial activity of Pistacia atlantica subsp. kurdica hulls' essential oil Food Bioscience, 100510

Hasheminya, S.-M., & Dehghannya, J. (2021). Development and characterization of novel edible films based on *Cordia dichotoma* gum

incorporated with *Salvia mirzayanii* essential oil nanoemulsion. *Carbohydrate Polymers, 257*, 117606.

Hasheminya, S.-M., Mokarram, R. R., Ghanbarzadeh, B., Hamishekar, H., & Kafil, H. S. (2018). Physicochemical, mechanical, optical, microstructural and antimicrobial properties of novel kefiran-carboxymethyl cellulose biocomposite films as influenced by copper oxide nanoparticles (CuONPs). *Food Packaging and Shelf Life, 17*, 196–204.

Hasheminya, S.-M., Mokarram, R. R., Ghanbarzadeh, B., Hamishekar, H., Kafil, H. S., & Dehghannya, J. (2019a). Influence of simultaneous application of copper oxide nanoparticles and *Satureja Khuzestanica* essential oil on properties of kefiran–carboxymethyl cellulose films. *Polymer Testing, 73*, 377–388.

Hasheminya, S.-M., Mokarram, R. R., Ghanbarzadeh, B., Hamishekar, H., Kafil, H. S., & Dehghannya, J. (2019b). Development and characterization of biocomposite films made from kefiran, carboxymethyl cellulose and *Satureja Khuzestanica* essential oil. *Food Chemistry, 289*, 443–452.

Hosseini, S. F., Zandi, M., Rezaei, M., & Farahmandghavi, F. (2013a). Two-step method for encapsulation of oregano essential oil in chitosan nanoparticles: Preparation, characterization and in vitro release study. *Carbohydrate Polymers, 95*(1), 50–56.

Hosseini, S. M., Hosseini, H., Mohammadifar, M. A., Mortazavian, A. M., Mohammadi, A., Khosravi-Darani, K., Shojaee-Aliabadi, S., Dehghan, S., & Khaksar, R. (2013b). Incorporation of essential oil in alginate microparticles by multiple emulsion/ionic gelation process. *International Journal of Biological Macromolecules, 62*, 582–588.

Hosseinnia, M., Khaledabad, M. A., & Almasi, H. (2013). Optimization of *Ziziphora clinopodiodes* essential oil microencapsulation by whey protein isolate and pectin: A comparative study. *Carbohydrate Polymers, 95*(1), 50–56.

Jemaa, M. B., Falleh, H., Serairi, R., Neves, M. A., Snoussi, M., Isoda, H., Nakajima, M., & Ksouri, R. (2018). Nanoencapsulated *Thymus capitatus* essential oil as natural preservative. *Innovative Food Science and Emerging Technologies, 45*, 92–97.

Jiang, S., Yildiz, G., Ding, J., Andrade, J., Rababahb, T. M., Almajwalc, A., Abulmeatyc, M. M., & Feng, H. (2019). Pea protein nanoemulsion and nanocomplex as carriers for protection of cholecalciferol (vitamin D_3). *Food and Bioprocess Technology, 12*, 1031–1040.

Lago, A. M. T., Neves, I. C. O., Oliveira, N. L., Botrel, D. A., Minim, L. A., & Resende, JVd. (2019). Ultrasound-assisted oil-in-water nanoemulsion produced from *Pereskia aculeata* Miller mucilage. *Ultrasonics Sonochemistry, 50*, 339–353.

Li, Y.-q, D-x, K., & Wu, H. (2013). Analysis and evaluation of essential oil components of cinnamon barks using GC–MS and FTIR spectroscopy. *Industrial Crops and Products, 41*, 269–278.

Li, Y., Li, M., Qi, Y., Zheng, L., Wu, C., Wang, Z., & Teng, F. (2020). Preparation and digestibility of fish oil nanoemulsions stabilized by soybean protein isolate-phosphatidylcholine. *Food Hydrocolloids, 100*, 105310.

Liu, T., & Liu, L. (2020). Fabrication and characterization of chitosan nanoemulsions loading thymol or thyme essential oil for the preservation of refrigerated pork. *International Journal of Biological Macromolecules, 162*, 1509–1515.

Lou, Z., Chen, J., Yu, F., Wang, H., Kou, X., Ma, C., & Zhu, S. (2017). The antioxidant, antibacterial, antibiofilm activity of essential oil from *Citrus medica* L. var. sarcodactylis and its nanoemulsion. *LWT-Food Science and Technology, 80*, 371–377.

Manea, A. M., Vasile, B. S., & Meghea, A. (2013). Antioxidant and antimicrobial activities of green tea extract loaded into nanostructured lipid carriers. *Comptes Rendus Chimie, 17*, 331–341.

Mehrabanjoubani, P., Nohooji, M. G., Karimi, E. & Abdolzadeh, A. (2021). The differences between *Froriepia subpinnata* (Ledeb.) Baill. and *Pimpinella anisum* L. commonly named as anarijeh based on major components of the essential oil; a marker for resolve ambiguities. *Journal of Medicinal Plants, 20*(79), 59–71.

Mendes, J. F., Martins, H. H. A., Otoni, C. G., Santana, N. A., Silvac, R. C. S., Silvad, A. G. D., Silvad, M. V., Correiad, M. T. S., Machadoc, G., Pinheiro, A. C. M., Piccoli, R. H., & Oliveira, J. E. (2018). Chemical composition and antibacterial activity of *Eugenia brejoensis* essential oil nanoemulsions against *Pseudomonas fluorescens*. *LWT-Food Science and Technology, 93*, 659–664.

Mirzania, F., Sarrafi, Y., & Farimani, M. M. (2019). Comparative evaluation of chemical compositions and biological activities of wild and cultivated *Froriepia subpinnata* L. essential oils. *Journal of Agricultural Science and Technology, 21*(2), 331–340.

Moghimi, R., Ghaderi, L., Rafati, H., Aliahmadi, A., Julian, D., & McClements, D. J. (2016). Superior antibacterial activity of nanoemulsion of *Thymus daenensis* essential oil against *E. coli*. *Food Chemistry, 194*, 410–415.

Mohammadzadeh, M., Mahmoudi, R., & Ghajarbeygi, P. (2018). Evaluation of chemical composition and antibacterial properties of *Froriepia subpinnta* essential oils from Guilan region: Before and after flowering. *Journal of Essential Oil Bearing Plants, 21*(4), 1119–1127.

Moraes-Lovison, M., Marostegan, L. F. P., Peres, M. S., Menezes, I. F., Ghiraldi, M., Rodrigues, R. A. F., Fernandes, A. M., & Pinho, S. C. (2017). Nanoemulsions encapsulating oregano essential oil: Production, stability, antibacterial activity and incorporation in chicken pate. *LWT-Food Science and Technology, 77*, 233–240.

Morteza-Semnani, K., Saeedi, M., & Akbarzadeh, M. (2009). The essential oil composition of Froriepia subpinnata (Ledeb.) Baill. *Journal of Essential Oil Research, 21*, 127–128.

Nirmal, N. P., Mereddy, R., Li, L., & Sultanbawa, Y. (2018). Formulation, characterisation and antibacterial activity of lemon myrtle and anise myrtle essential oil in water nanoemulsion. *Food Chemistry, 254*, 1–7.

Noori, S., Zeynali, F., & Almasi, H. (2018). Antimicrobial and antioxidant efficiency of nanoemulsion-based edible coating containing ginger (*Zingiber officinale*) essential oil and its effect on safety and quality attributes of chicken breast fillets. *Food Control, 84*, 312–320.

Pires, A. M. L., Albuquerque, M. R. J. R., Nunes, E. P., Melo, V. M. M., Silveira, E. R., & Pessoa, O. D. L. (2006). Chemical composition and antibacterial activity of the essential oils of *Blainvillea rhomboidea* (Asteraceae). *Natural Product Communications, 1*, 395–398.

Rustaiyan, A., Mojab, R., Kazemie-Piersara, M., Bigdeli, M., Masoudi, S. & Yari, M. (2001). Essential oil of *Froriepia subpinnata* (Ledeb.) Baill. from Iran. *Journal of Essential Oil Research, 13*(6), 405–406.

Sadowska, U., Matwijczuk, A., Niemczynowicz, A., Dróżdż, T., & Żabiński, A. (2019). Spectroscopic examination and chemometric analysis of essential oils obtained from peppermint herb (*Mentha piperita* L.) and caraway fruit (*Carum carvi* L.) subjected to pulsed electric fields. *Processes, 7*(7), 466.

Safaya, M., & Rotliwala, Y. (2022). Neem oil based nano-emulsion formulation by low energy phase inversion composition method: Characterization and antimicrobial activity. *Materials Today: Proceedings, 57*, 1793–1797.

Salvia-Trujillo, L., Rojas-Grau, A., Soliva-Fortuny, R., & Martin-Belloso, O. (2013). Physicochemical characterization of lemongrass essential oil–alginate nanoemulsions: Effect of ultrasound processing parameters. *Food and Bioprocess Technology, 6*, 2439–2446.

Sandri, I. G., Zacaria, J., Fracaro, F., Delamare, A. P. L., & Echeverrigaray, S. (2007). Antimicrobial activity of the essential oils of Brazilian species of the genus Cunila against foodborne pathogens and spoiling bacteria. *Food Chemistry, 103*(3), 823–828.

Santos, MKd., Kreutz, T., Danielli, L. J., Marchi, J. G. B. D., Pippi, B., Koester, L. S., Fuentefria, A. M., & Limberger, R. P. (2020). A chitosan hydrogel-thickened nanoemulsion containing *Pelargonium graveolens* essential oil for treatment of vaginal candidiasis. *Journal of Drug Delivery Science and Technology, 56*, 101527.

Sepahvand, S., Amiri, S., Radi, M., & Akhavan, H.-R. (2021). Antimicrobial activity of thymol and thymol-nanoemulsion against three food-borne pathogens inoculated in a sausage model. *Food and Bioprocess Technology, 14*, 1936–1945.

Shahavi, M. H., Hosseini, M., Jahanshahi, M., Meyer, R. L., & Darzi, G. N. (2015). Evaluation of critical parameters for preparation of stable clove oil nanoemulsion. *Arabian Journal of Chemistry*.

Shahavi, M. H., Hosseini, M., Jahanshahi, M., Meyer, R. L., & Darzi, G. N. (2016). Clove oil nanoemulsion as an effective antibacterial agent: Taguchi optimization method. *Desalination and Water Treatment, 57*(39), 18379–18390.

Shetta, A., Kegere, J., & Mamdouh, W. (2019). Comparative study of encapsulated peppermint and green tea essential oils in chitosan nanoparticles: Encapsulation, thermal stability, in-vitro release, antioxidant and antibacterial activities. *International Journal of Biological Macromolecules, 126*, 731–742.

Sivakumar, M., Tang, S. Y., & Tan, K. W. (2014). Cavitation technology - a greener processing technique for the generation of pharmaceutical nanoemulsions. *Ultrasonics Sonochemistry, 21*, 2069–2083.

Sreejayan, N., & Rao, M. N. (1996). Free radical scavenging activity of curcuminoids. *Drug Research, 46*, 169–171.

Sugumar, S., Ghosh, V., Nirmala, M. J., Mukherjee, A., & Chandrasekaran, N. (2014). Ultrasonic emulsification of eucalyptus oil nanoemulsion: Antibacterial activity against Staphylococcus aureus and wound healing activity in Wistar rats. *Ultrasonics Sonochemistry, 21*, 1044–1049.

Tamjidi, F., Shahedi, M., Varshosaz, J., & Nasirpour, A. (2013). Nanostructured lipid carriers (NLC): A potential delivery system for bioactive food molecules. *Innovative Food Science and Emerging Technologies, 87*, 21–43.

Tiwari, S., Upadhyay, N., Singh, B. K., Singh, V. K., & Dubey, N. K. (2022). Facile fabrication of nanoformulated *Cinnamomum glaucescens* essential oil as a novel green strategy to boost potency against food borne fungi, aflatoxin synthesis, and lipid oxidation. *Food and Bioprocess Technology*.

Wang, Y., Cen, C., Chen, J., Zhou, C., & Fu, L. (2021). Nano-emulsification improves physical properties and bioactivities of *litsea cubeba* essential oil. *LWT-Food Science and Technology, 137*, 110361.

Yukuyama, M. N., Ghisleni, D. D. M., Pinto, T. J. A., & Bou-Chacra, N. A. (2015). Nanoemulsion: Process selection and application in cosmetics - a review. *International Journal of Cosmetic Science, 38*(1), 13–24.

Zhu, Z., Zhao, C., Yi, J., Cui, L., Liu, N., Cao, Y., & Decker, E. A. (2018). Ultrasound improving the physical stability of oil-in-water emulsions stabilized. *Journal of the Science of Food and Agriculture, 98*(11), 4323–4330.

Ziani, K., Fang, Y., & McClements, D. J. (2012). Fabrication and stability of colloidal delivery systems for flavor oils: Effect of composition and storage conditions. *Food Research International, 46*, 209–216.